Published in final edited form as:
J Mol Cell Cardiol. 2014 January ; 66: 27–40. doi:10.1016/j.yjmcc.2013.10.010.

The C-terminus of the long AKAP13 isoform (AKAP-Lbc) is critical for development of compensatory cardiac hypertrophy

Domenico M. Taglieri, MD, PhD[1], **Keven R. Johnson, PhD**[1], **Brian T. Burmeister, BSc**[1], **Michelle M. Monasky, PhD**[2,3], **Matthew J. Spindler, PhD**[4], **Jaime DeSantiago, MD, PhD**[3], **Kathrin Banach, PhD**[3], **Bruce R. Conklin, MD**[4], and **Graeme K. Carnegie, PhD**[1,#]

[1]Department of Pharmacology, University of Illinois at Chicago, Chicago, 60612, Illinois, USA

[2]Department of Physiology and Biophysics, University of Illinois at Chicago, Chicago, 60612, Illinois, USA

[3]Center for Cardiovascular Research, College of Medicine, University of Illinois at Chicago, Chicago, 60612, Illinois, USA

[4]Gladstone Institute of Cardiovascular Disease, 1650 Owens Street, San Francisco, CA 94158, USA.

Abstract

The objective of this study was to determine the role of A-Kinase Anchoring Protein (AKAP)-Lbc in the development of heart failure, by investigating AKAP-Lbc-protein kinase D1 (PKD1) signaling *in vivo* in cardiac hypertrophy.

Using a gene-trap mouse expressing a truncated version of AKAP-Lbc (due to disruption of the endogenous AKAP-Lbc gene), that abolishes PKD1 interaction with AKAP-Lbc (AKAPLbc-ΔPKD), we studied two mouse models of pathological hypertrophy: i) angiotensin (AT-II) and phenylephrine (PE) infusion and ii) transverse aortic constriction (TAC)-induced pressure overload.

Our results indicate that AKAP-Lbc-ΔPKD mice exhibit an accelerated progression to cardiac dysfunction in response to AT-II/PE treatment and TAC. AKAP-Lbc-ΔPKD mice display attenuated compensatory cardiac hypertrophy, increased collagen deposition and apoptosis, compared to wild-type (WT) control littermates. Mechanistically, reduced levels of PKD1 activation are observed in AKAP-Lbc-ΔPKD mice compared to WT mice, resulting in diminished phosphorylation of histone deacetylase 5 (HDAC5) and decreased hypertrophic gene expression. This is consistent with a reduced compensatory hypertrophy phenotype leading to progression of

[#]**Correspondence to:** Graeme K. Carnegie, Ph.D. Department of Pharmacology College of Medicine University of Illinois at Chicago 835 S. Wolcott Avenue Chicago, IL 60612-7342 Phone: 312-355-4435 carnegie@uic.edu.

8. DISCLOSURES
None.

heart failure in AKAP-Lbc-ΔPKD mice. Overall, our data demonstrates a critical *in vivo* role for AKAP-Lbc-PKD1 signaling in the development of compensatory hypertrophy to enhance cardiac performance in response to TAC-induced pressure overload and neurohumoral stimulation by AT-II/PE treatment.

Keywords

A-Kinase Anchoring Protein (AKAP); protein kinase D; cardiac hypertrophy; heart failure.

1. INTRODUCTION

Localized regulation and integration of intracellular signal transduction is important for cardiac function. Disruption of appropriate signaling results in development of heart failure [1-2]. A-kinase anchoring proteins (AKAPs) are fundamental regulatory molecules involved in signal transduction, functioning to target unique signaling complexes to distinct subcellular locations, thereby coordinating signaling and generating substrate specificity [3]. In the heart, AKAPs play a crucial role by integrating cAMP-dependent protein kinase (protein kinase A; PKA) signaling with additional enzymes to modulate physiological functions, including Ca^{2+}-cycling and cardiac contractility [4], as well as pathological processes involved in cardiac remodeling and the development of heart failure [5]. Subcellular localization of signaling components by AKAPs is important for cardiac function. Multiple AKAPs have been identified in cardiac myocytes, targeting signaling complexes to distinct subcellular regions including the sarcolemma [6], sarcoplasic reticulum [7], nuclear envelope [8], and sarcomere [9-11].

A recent proteomic study suggests that differential expression of AKAPs coupled with alterations in the AKAP “interactome” may be critical factors in heart failure [12], however currently, few AKAP knockout or transgenic mouse models have been studied to specifically determine *in vivo* (patho)physiological roles in healthy and diseased heart. Here, we focus on the *in vivo* role of the *AKAP13* gene long transcript, called AKAP-Lbc; due to an N-terminal AKinase Anchoring domain [13] and a C-terminal region originally identified in a screen for transforming genes from human myeloid leukemia patients in Lymphoid Blast Crisis [14]. AKAP-Lbc serves as a scaffold for multiple protein kinases, including PKA, protein kinase C (PKCα and PKCη isoforms) and protein kinase D (PKD1) [15]. AKAP-Lbc also acts as a guanine exchange factor (GEF) for Rho [13] and mediates activation of p38α MAPK [16], ERK1/2 [17] and IκB kinase β (IKKβ) [18]. Additionally, we have recently demonstrated that AKAP-Lbc tethers the tyrosine phosphatase Shp2; which is inhibited by PKA phosphorylation in the AKAP-Lbc complex under hypertrophic conditions in the heart [19]. AKAP-Lbc is predominantly expressed in the heart [13] and is essential for cardiac function. Knockout of AKAP-Lbc in mice leads to embryonic lethality due to decreased expression of cardiac developmental genes and deficient sarcomere formation in developing myocytes, resulting in a thin myocardium in the developing heart [20]. Previously, we and others have demonstrated a role for AKAP-Lbc in the induction of cardiac hypertrophy *in vitro* [21] [22]. Cardiac myocytes primarily respond to increased workload by an increase in size (hypertrophy). Initially cardiac hypertrophy is a beneficial,

compensatory process, decreasing wall stress and increasing cardiac output and stroke volume. However, prolonged hypertrophy is maladaptive, transitioning to decompensation and cardiac failure [23] [24]. Understanding how molecular events are orchestrated by AKAP-Lbc may lead to the identification of new pharmacological approaches for treatment of heart failure.

AKAP-Lbc expression is upregulated in hypertrophic neonatal rat ventricular myocytes (NRVM), whereas siRNA-silencing of AKAP-Lbc expression reduces phenylephrine (PE)-stimulated expression of hypertrophic markers and hypertrophy [21] [22]. A similar increase in AKAP-Lbc expression was also observed in human heart specimens obtained from patients with hypertrophic cardiomyopathy where AKAP-Lbc mRNA content was increased, compared to control age-matched healthy human heart samples [21].

In knockdown/rescue experiments using NRVM, to dissect signaling through AKAP-Lbc, our results show that AKAP-Lbc scaffolding of PKD1 is the predominant mechanism of AKAPLbc-mediated hypertrophy [21]. Mechanistically, AKAP-Lbc facilitates activation of PKD1 (the predominant protein kinase D cardiac isoform [25-27]) in response to hypertrophic stimuli including PE and endothelin-1 (ET-1). AKAP-Lbc contributes to PKD1 activation in two ways: first, by bringing PKC and PKD1 into close proximity, thereby facilitating phosphorylation and activation of PKD1 by PKC. Second, PKA phosphorylation of AKAP-Lbc, in the PKD1 binding region of AKAP-Lbc (at S2737) releases newly activated PKD1 from the AKAP-Lbc complex. Thus, AKAP-Lbc-anchored PKC and PKA synergistically activate PKD1 by promoting activation and passage of multiple PKD1 molecules through AKAP-Lbc [14].

Activation of PKD1 through AKAP-Lbc facilitates phosphorylation and subsequent nuclear export of histone deacetylase 5 (HDAC5) [21], leading to de-repression of the transcription factor MEF2, resulting in cardiac myocyte hypertrophy through MEF2-mediated transcription of muscle-specific genes and re-expression of developmental genes [28] [29]. Currently, the *in vivo* role of this signaling pathway is unknown. Therefore, we set out to determine the role of AKAP-Lbc-PKD1 in the context of pathological hypertrophy and the development of heart failure. In this report, we utilize a gene-trap mouse expressing a form of AKAP-Lbc that is truncated at the C-terminus and unable to bind PKD1. AKAP-Lbc-ΔPKD mice are viable, displaying normal cardiac structure and electrocardiograms. AKAP-Lbc-PKD1 signaling does not appear to be critical for development, but may play a minor role under conditions of β-adrenergic (predominantly Gs-Protein-Coupled Receptor)-induced cardiac hypertrophic remodeling. In response to isoproterenol treatment, mice lacking both the GEF and PKD-binding domains of AKAP-Lbc display abnormal cardiac contractility despite a similar increase in heart size, compared to control wild-type (WT) mice [30].

Here, we demonstrate an *in vivo* role for AKAP-Lbc in the induction of compensatory myocardial hypertrophy in response to pressure overload and angiotensin-II/phenylephrine (ATII/PE) treatment, both known to activate PKD1, predominantly via Gq-PCR mediated pathways.

2. MATERIALS AND METHODS

2.1. Generation of the *AKAP-Lbc-ΔPKD Mouse*

The AKAP-Lbc-ΔPKD mouse was generated from MMRRC gene-trap ES cell line CSJ288 (strain genetic background: B6NCr.129P2) on a C57Bl/6 background and is fully described in [30]. The gene-trap construct uses a strong splice acceptor to create a fused mRNA of upstream AKAP-Lbc exons with the trapping cassette [31]. The AKAP-Lbc-ΔPKD truncation mutant results from specific integration of a β-Geo cassette (β-Galactosidase/neomycin resistance gene) within the endogenous AKAP-Lbc genomic locus, therefore the truncated AKAP-Lbc-β-Geo fusion protein is expressed from the endogenous upstream AKAP-Lbc gene promoter. RT-PCR and sequencing from ES cells and homozygous gene-trap mice confirmed specific gene-trap targeting within the AKAP-Lbc gene.

2.2. Antibodies

Anti-phospho-HDAC4 (Ser246)/HDAC5 (Ser259)/HDAC7 (Ser155) (D27B5) (#3443), anti-HDAC5 (#2082) and anti-PKD1/PKCμ (#2052) were from Cell Signaling Technology, Inc. Anti-cTnI (ab19615) was from AbCam.

2.3. In Vitro Protein Kinase Assay

Immune complexes were washed five times with IP buffer (10 mM sodium phosphate, pH 6.95, 150 mM NaCl, 5 mM EDTA, 5 mM EGTA, 1% Triton X-100) and then resuspended in kinase assay buffer (50 mM Tris-HCl, pH 7.5, 5 mM $MgCl_2$). Assays were performed as described in [32]. PKD activity assays were carried out using a total reaction volume of 50 μl including 100 μM syntide-2, 5 μM ATP, 5 μCi of [γ-^{32}P]-ATP in kinase assay buffer. Reactions were for 20 min at 30°C, started upon addition of ATP. Reactions were terminated by centrifugation followed by spotting the reaction mix (40 μl) onto P81 phosphocellulose paper (Whatman). Phosphocellulose papers were washed three times with 75 mM phosphoric acid, once with acetone and then dried. Kinase activity was determined by liquid scintillation counting. PKA activity assays were performed as described for PKD. Prior to assay, PKA catalytic subunit was eluted from AKAP-Lbc immune complexes by adding 50 μl of 10 mM cAMP and incubating for 20 min. PKA assays were carried out in a total reaction volume of 50 μl, using 20 μl of eluted PKA catalytic subunit, 200 μM Kemptide, 5 μM ATP, 5 μCi of [γ-^{32}P]-ATP in kinase assay buffer.

2.4. In Vitro Rho-Guanine Exchange Factor (GEF) Assay

Following immunoprecipitation of AKAP-Lbc, immune complexes were washed five times with IP buffer and incubated with RhoA-GDP (40 pmol) in binding buffer (50 mM Tris-HCl, pH 7.5, 1 mM DTT, 0.5 mM EDTA, 50 mM NaCl, 5 mM $MgCl_2$, 0.05% polyoxyethylene-10-lauryl ether ($C_{12}E_{10}$), and 10 μM GTPγS with ~500 cpm/pmol [^{35}S]-GTPγS) in a final reaction volume of 50 μl. Reactions were terminated after 20 min incubation at 30°C by addition of wash buffer. GTPγS binding to RhoA was determined as previously described [33]. [^{35}S]-GTPγS (specific activity = 1,250 Ci/mmol) was obtained from PerkinElmer Life Sciences.

2.5. Systemic Blood Pressure Measurement

Intraventricular hemodynamic measurements were carried out using a Scisense FY097B pressure-volume hemodynamics system. Mice were intubated with a 20G angiocath sleeve, connected to a mouse ventilator supplying 1.5% isoflurane mixed with 100% oxygen (Vent settings: Resp rate ≈ 150 bpm and Tidal volume ≈ 150 microliters) and then placed supine on a heated pad (37.5° C). A pressure catheter was inserted in the carotid artery towards the left ventricle. 6 (1 month old) AKAP-Lbc-ΔPKD mice and 5 WT control littermates were used.

2.6. Isolation of Adult Ventricular Myocytes (VM's)

Isolation of VM's from AKAP-Lbc-ΔPKD mice and WT control littermates was carried out as previously described [34]. Briefly, adult mice were anesthetized in a gas chamber with 3-5% isoflurane (100% O_2), hearts were excised and mounted on a Langendorff-perfusion apparatus and perfused at 3 ml/min with Ca^{2+}-free Tyrode's solution for 6 min at 37 °C. Perfusion was then switched to Ca^{2+}-free Tyrode's solution containing 0.1 mg/ml Liberase TM (Roche) until the heart became flaccid (7-12 min). Ventricular tissue was removed, dispersed, filtered, and suspensions rinsed several times (while gradually increasing [Ca^{2+}] to 1 mM). Myocytes were plated on coverslips pre-coated with laminin (GIBCO, Grand Island, NY).

2.7. Mouse Models of LV Concentric Cardiac Hypertrophy

Osmotic minipumps were used to deliver G protein coupled receptor (GPCR)-agonists: AT-II and PE, as previously described [35] and transverse aortic constriction (TAC) was carried out to promote pressure overload-induced cardiac hypertrophy [36]. All experiments were approved in accordance with the UIC Animal Care and Use Committee. Before surgery, mice were anesthetized with sodium pentobarbital (100 mg/kg, ip), placed on a ventilator (Harvard Rodent Ventilator, Harvard Apparatus, Holliston, MA) and core temperature was maintained at 37°C with a heating pad. Stenosis of the transverse aorta was measured using anatomic M-mode echocardiography from mice with satisfactory echocardiographic images of the aortic arch. Percent stenosis was ~65% in mice receiving TAC surgery (calculated as the difference between the normal luminal area and the stenosed area, divided by the normal luminal area). 48 age-matched, 3-4 month-old, C57BL/6 male and female mice (24 WT and 24 AKAP-Lbc-ΔPKD) were randomized into 8 groups of 6 mice each to receive: i) continuous subcutaneous administration of 1 μg/g/day of AT-II and 100 mg/kg/day of PE in the same osmotic minipump; or ii) an equivalent volume of 0.91% w/v NaCl (saline) for 4 weeks (end of study), iii) transverse aortic constriction (TAC), or iv) sham transverse aortic constriction, for 4 weeks (end of study). For appropriate comparison, the numbers of each sex, across study groups were kept consistent. WT + saline (4 females, 2 males); WT + AT-II/PE (4 females, 2 males); AKAP-Lbc-ΔPKD + saline (4 females, 2 males); AKAP-Lbc-ΔPKD + ATII/PE (4 females, 2 males). WT/Sham (3 females, 3 males); WT/TAC (3 females, 3 males); AKAP-Lbc-ΔPKD/Sham (3 females, 3 males); AKAP-Lbc-ΔPKD/TAC (3 females, 3 males) were generated. At the end of the study, mice were sacrificed and heart and body weights obtained. Hearts were then stored at −80°C for morphometric, biochemical, and histochemical analyses.

2.8. Transthoracic M-Mode and Pulsed Doppler Echocardiography

Echocardiographic measurements were performed for all experimental groups, before and 30 days after mini-osmotic pump implantation or TAC. Mice were initially anesthetized with 3% isoflurane and 100% oxygen inhaled in a closed anesthesia chamber. A plane of anesthesia was then regulated by delivery of 1% isoflurane administered through a nose cone with 100% oxygen. Mice were placed in the dorsal decubitus position on a warming pad to maintain normothermia. Transthoracic two-dimensional, M-mode and pulsed Doppler images were acquired with a high-resolution echocardiographic system (VeVo 770, Visual Sonics, Toronto, ON, Canada) equipped with a 30-MHz mechanical transducer. All measurements were taken in compliance with the American Society of Echocardiography guidelines [37]. Results are based on the average of at least three cardiac cycles.

2.9. Hydroxyproline (HOP) Assay

Hydroxyproline (HOP) content was determined from mouse cardiac tissue using a wet weight of 15-20 mg. Samples were hydrolyzed overnight in 200μl of 12M HCl at 110°C, in glass vials. After hydrolysis, 80 μl of isopropanol was added to 5 μl of hydrolysate, followed by 40 μl of chloramine-T solution (7% chloramine-T in water) mixed with acetate citrate buffer (0.695M anhydrous $C_2H_3O_2Na$, 0.174M $C_6H_8O_7$, 0.435M NaOH, and 38.5% [v/v] 2-propanol) in a 1:4 ratio. Samples were vortexed, and allowed to oxidize for 5 min at room temperature. 0.5 ml of Ehrlich's regent (3g of 4-(dimethylamino) benzaldehyde, 10 ml ethanol, 675 μl sulfuric acid) mixed with 2-propanol in a 3:13 ratio was added, vortexed, and incubated for 30 min at 55°C, then quenched in an ice bath. Following centrifugation at 5,000×g for 1 min the supernatant optical density was determined at 558 nm. A standard curve of *trans*-4-hydroxy-L-proline (0– 500 nM) was included in each assay for calibration of HOP concentration (μM HOP/mg of tissue).

2.10. Histologic Analysis and TUNEL Assay

Hearts were fixed in 4% paraformaldehyde for 48 h, and processed in paraffin. Paraffin-embedded sections were stained with hematoxylin-eosin and Picro-Sirius Red Fast Green. Fibrotic areas stained red and normal tissue stained light green. Apoptosis was examined using the terminal deoxynucleotidyltransferase-mediated dUTP nick end labeling (TUNEL) assay (In Situ Cell Death Detection Kit, Roche Applied Science). TUNEL-positive nuclei in heart sections were counted from 1,000 cells total per group, using 3 mice per group, over at least 3 different sections per mouse. Images were acquired using an LSM 510 mounted on an Axiovert 100 M microscope (Carl Zeiss Co., Ltd.).

2.11. Quantitative PCR Analysis

Total RNA was extracted from frozen mouse cardiac tissue using Trizol (Molecular Research Center, Cincinnati, OH, USA). Random-primed, reverse transcribed cDNA synthesis reactions were performed using SuperScript III Reverse transcriptase (Invitrogen Corporation). Forward and reverse primers for βGeo, mouse AKAP-Lbc, NAD subunit 6, alpha-actinin, myosin heavy chain-alpha, myosin heavy chain-beta, ANP, BNP, and GAPDH were generated based on previously published primer pairings available at PrimerBank (http://pga.mgh.harvard.edu/primerbank/index.html) or Real Time PCR Primer

Sets (http://www.realtimeprimers.org/). Primers were analyzed for secondary structure formation using IDT SciTools (www.idtdna.com). Target amplicons were selected between 100 and 150 base pairs with at least one primer spanning an exon junction. Final concentrations of sense and antisense primers were determined for each primer pair based on optimal amplification efficiency and melt curve analysis. Primers are listed in Supplemental Table 7. Reactions were carried out with Power SYBR-green PCR mix (Life Technologies) using an Applied Biosystems ViiA7 Real Time PCR system. The Ct (defined as the cycle number at which the fluorescence exceeds the threshold level) was determined for each reaction and quantification was determined using the ΔΔCt method [38]. The target Ct was determined for each sample and then normalized to the GAPDH mRNA Ct from the same sample. These values were then compared with control levels using the $2^{-\Delta\Delta Ct}$ method and represented as fold difference normalized to the appropriate control sample (i.e., wild-type sham surgery or saline infusion).

2.12. Statistics

Data are expressed as mean ± standard error of the mean (SEM). Differences in quantitative variables were determined using two-way analysis of variance (ANOVA) followed by Bonferroni's Multiple Comparison Test student's t test for comparison between multiple groups, or by unpaired t test for comparison between two groups. Significant *P* values are referred as follows: (*) denotes a P value < 0.05, (**) denotes a P value < 0.01 and (***) denotes a P value < 0.001. All analyses were performed using GraphPad Prism, JMP or InStat statistical software.

3. RESULTS

3.1. Characterization of AKAP-Lbc-ΔPKD

Figure 1A shows a diagram of AKAP-Lbc-ΔPKD, which is expressed in the gene-trap mouse, developed from Mutant Mouse Regional Resource Ceter (MMRRC) gene-trap embryonic stem cell line CSJ288. AKAP-Lbc-ΔPKD refers to a truncated form of AKAP-Lbc that cannot bind PKD1 (as demonstrated by the Western blot in Fig. 1D showing co-immunoprecipitation of endogenous PKD1 with AKAP-Lbc-WT, but not AKAP-Lbc-ΔPKD. Generation and initial characterization of AKAP-Lbc-ΔPKD mice, as well as extensive characterization of AKAP-Lbc-ΔPKD using a corresponding construct expressed in HEK293 cells is reported in [30]. Importantly, the AKAP-Lbc-ΔPKD truncation mutant results from specific integration of the β-Geo cassette within the endogenous AKAP-Lbc genomic locus, thus the truncated AKAP-Lbc-β-Geo fusion protein is expressed from the endogenous upstream AKAP-Lbc gene promoter. Therefore, AKAP-Lbc-ΔPKD message and protein levels in gene-trap mouse tissue are similar to that of full-length AKAP-Lbc in wild-type mice. To quantify AKAP-Lbc expression we performed Real-Time (RT)-PCR analysis of atrial and ventricular samples from AKAP-Lbc-ΔPKD mice and control wild-type littermates; Figs. 1B & C). Consistent with previous X-Gal staining [30], our results indicate that both AKAP-Lbc-(WT) and AKAP-Lbc-ΔPKD are similarly expressed with higher levels in the atria compared to ventricles. Ventricular message levels correspond to 65 ± 0.4% of that in the atria. A control RT-PCR was carried out using βGeo specific primers indicating similar relative atrial and ventricular levels of AKAP-Lbc-ΔPKD

expression when compared to the AKAP-Lbc-specific primer set used in Fig. 1B. As expected, there was no βGeo expression in WT hearts (Fig. 1C).

We measured endogenous PKA and PKD activity associated with AKAP-Lbc-ΔPKD and AKAP-Lbc-WT by immunoprecipitation of AKAP-Lbc and *in vitro* kinase assay from corresponding mouse heart lysates. No differences are observed in expression levels of AKAPLbc-ΔPKD, compared to AKAP-Lbc-WT, however PKD activity associated with endogenous AKAP-Lbc (-ΔPKD) from AKAP-Lbc-ΔPKD gene trap mouse heart lysate is abolished, compared to that associated with endogenous wild-type AKAP-Lbc from wild-type (WT) control mouse heart lysate (Fig. 1D). No differences are observed in AKAP-Lbc associated PKA activity from either AKAP-Lbc-ΔPKD or AKAP-Lbc-WT mouse heart lysates (Fig. 1E). Western blot analysis support the kinase assay results, indicating that endogenous PKA and PKD1 coimmunoprecipitate with AKAP-Lbc-WT, whereas PKA, but not PKD1 co-immunoprecipitates with AKAP-Lbc-ΔPKD (Figs. 1D & E). It should be noted that the expected predicted difference in size between the AKAP-Lbc-WT and AKAP-Lbc-ΔPKD is not differentiated using 8% SDS-PAGE. Measurement of total PKD activity from AKAP-Lbc-ΔPKD mouse heart lysates is reduced, compared to that in AKAP-Lbc-WT mouse heart lysates. Under basal conditions, there is a ~30% reduction in total PKD activity in AKAP-Lbc-ΔPKD heart lysate compared to WT (Fig. 1F). As expected, no differences are observed in total PKA activity from AKAP-Lbc-ΔPKD and AKAP-Lbc-WT mouse heart lysates (Fig. 1G). Overall, these data indicate that PKD binding to AKAP-Lbc is critical in promoting a significant pool of PKD activity in the heart.

Based on literature suggesting that the C-terminus of AKAP-Lbc also regulates intrinsic Rho-guanine exchange factor (GEF) activity [39] we measured AKAP-Lbc Rho-GEF activity. No differences are observed in the Rho-GEF activity of AKAP-Lbc-ΔPKD, compared to full-length AKAP-Lbc-WT from mouse heart lysates (Fig. 1H).

Thus overall, the AKAP-Lbc-ΔPKD mouse provides a good model to define the *in vivo* role(s) of AKAP-Lbc-regulated PKD1.

3.2. AKAP-Lbc-ΔPKD mice fail to develop compensatory cardiac hypertrophy from chronic stress by AT-II/PE infusion or TAC-induced pressure overload

Heart weight (HW) to body weight (BW) measurements and results from echocardiographic analysis are presented in Figures 2, 3, Supplemental Figures 1-3 and Supplemental Tables 1-4.

Under basal conditions, no statistically significant differences in cardiac dimensions and function exist between AKAP-Lbc-ΔPKD mice and control wild-type littermates (WT) at 8 weeks old, and in mice aged 50-61 weeks (Supp. Table 5).

In response to AT-II/PE treatment, WT mice develop a statistically significant increase in HW/BW compared to AKAP-Lbc-ΔPKD mice (Fig. 2A). AKAP-Lbc-ΔPKD mice exhibit attenuated cardiac hypertrophy (LV mass increase of 21.8 ± 4.2%), compared to control WT littermates (LV mass increase of 94.8 ± 8.2%), (Supp. Figs. 1A & B). WT mice exhibit a significant increase in LV posterior and anterior wall thickness, compared to AKAP-Lbc-

ΔPKD mice (Fig. 2B & Supp. Fig. 1C). Unlike WT mice, AKAP-Lbc-ΔPKD mice display minimal changes in LV performance in response to AT-II/PE treatment (Fig. 2C). Overall, these results suggest that WT mice develop concentric hypertrophy in response to AT-II/PE administration for 30 days. This was not evident in the AKAP-Lbc-ΔPKD mice.

We also examined cardiac dimensions and function in AKAP-Lbc-ΔPKD mice and control WT littermates at baseline and after 30 days of TAC (or sham) surgery (Fig. 3 & Supp. Fig. 2). No significant differences among control sham surgery groups were observed. Similar to the AT-II/PE study, we found that AKAP-Lbc-ΔPKD mice display reduced cardiac hypertrophy in response to TAC, compared to WT control mice. Results show reduced increase in heart weight to body weight ratio (Fig. 3A), LV mass (Supp. Figs. 2A & B) and LV posterior and anterior wall dimensions (Fig. 3B & Supp. Fig. 2C respectively). In response to TAC, AKAP-Lbc-ΔPKD mice develop a 52.5 ± 13.1% increase in LV mass, while WT mice develop a 115.5 ± 22.1% increase (Supp. Fig. 2B). Both AKAP-Lbc-ΔPKD and WT control littermates develop systolic dysfunction, indicated by decreased LV EF (Fig. 3C). LV EF is significantly decreased in AKAP-Lbc-ΔPKD mice compared to WT control littermates following TAC, indicating greater severity of cardiac dysfunction in AKAP-Lbc-ΔPKD mice in response to pressure overload. A restrictive filling pattern is observed in AKAP-Lbc-ΔPKD mice, demonstrated by a significantly increased E/A ratio (Fig. 3D), indicating diastolic dysfunction. LV chamber internal diameter is increased in AKAP-Lbc-ΔPKD mice, suggesting that AKAP-Lbc-ΔPKD mice develop eccentric hypertrophy in response to TAC, whereas WT mice develop concentric hypetrophy after TAC. These findings were confirmed post-mortem, by examining heart sections at the mid-papillary level (Fig. 3E).

Overall, our results demonstrate that unlike WT control mice, AKAP-Lbc-ΔPKD mice do not develop concentric hypertrophy associated with preserved cardiac function, in response to cardiac stress (AT-II/PE treatment and TAC). AKAP-Lbc-ΔPKD mice develop an attenuated increase in LV mass with no change in systolic and diastolic function in response to AT-II/PE treatment. AKAP-Lbc-ΔPKD mice develop severe eccentric hypertrophy with compromised systolic and diastolic function in response to TAC-induced pressure overload. These results determine a critical role for the C-terminus of AKAP-Lbc in the induction of compensatory hypertrophy in response to cardiac stress.

3.3. AKAP-Lbc-ΔPKD mice exhibit no difference in blood pressure compared to WT control littermates

AKAP-Lbc is predominantly expressed in cardiac tissue, but is also present in other tissue, including the vasculature. Recent data from a Genome-Wide Association Study (GWAS) in a Korean population has linked high blood pressure with a single nucleotide polymorphism (SNP) in the GATA-3 transcription factor binding promoter region of the *AKAP13* gene [40]. Therefore, we wondered if blood pressure was affected in the AKAP-Lbc-ΔPKD mice compared to WT control littermates and whether this might affect the development of cardiac hypertrophy and heart failure in the AKAP-Lbc-ΔPKD mice. Results show that under basal conditions there is no difference in blood pressure between AKAP-Lbc-ΔPKD mice compared to WT control littermates (Supp. Table 6). Importantly, these data suggest

that the AKAP-Lbc-ΔPKD mice are not pre-disposed to develop heart failure compared to the WT control mice due to a difference (increase) in blood pressure.

3.4. AKAP-Lbc-ΔPKD mice exhibit reduced myocyte hypertrophy with increased cardiac extracellular collagen synthesis and apoptosis, in response to TAC-induced pressure overload or AT-II/PE infusion

Histologic analysis by hematoxylin/eosin (H/E) staining of LV sections indicates reduced myocyte hypertrophy in AKAP-Lbc-ΔPKD mice compared to WT mice in response to TAC (Fig. 4A) or AT-II/PE (Supp. Fig. 4A). This result is confirmed by width and length measurements of ventricular myoctes isolated from AKAP-Lbc-ΔPKD and WT mouse hearts after TAC and sham surgery (Figs 4B-E). Myocytes isolated from WT mice + TAC exhibit increased cell size (both width and length) compared to myocytes from AKAP-Lbc-ΔPKD mice + TAC. No difference was observed between AKAP-Lbc-ΔPKD and WT mice under sham conditions (Figs. 4B-E). These data indicate that development of myocyte hypertrophy in response to TAC is diminished in AKAP-Lbc-ΔPKD mice compared to WT control littermates.

Additionally, Sirius Red staining of LV sections indicates increased fibrosis in AKAP-Lbc-ΔPKD hearts subjected to TAC (Fig. 4F), or treatment with AT-II/PE (Supp. Fig 4B). This observation was confirmed by hydroxyproline (HOP) assay quantifying collagen content from mice hearts subjected to TAC (Fig. 4G) and AT-II/PE treatment (Supp. Fig 4C). Average HOP content (± SEM) was 5.4 ± 0.5 μM/mg for WT/sham; 4.3 ± 1.3 μM/mg for WT/TAC; 4.3 ± 1.4 μM/mg for AKAP-Lbc-ΔPKD/sham and 6.2 ± 1.6 μM/mg for AKAP-Lbc-ΔPKD/TAC (n=3 for all groups). Average HOP content (± SEM) was 3.3 ± 0.2 μM/mg for WT + saline; 3.0 ± 0.1 μM/mg for WT + AT-II/PE; 2.6 ± 0.2 μM/mg for AKAP-Lbc-ΔPKD + saline and 4.3 ± 0.6 μM/mg for AKAP-Lbc-ΔPKD + ATII/PE (n=3 for all groups).

Reduced cellularity and increased extracellular space is exhibited in LV sections from AKAP-Lbc-ΔPKD mice subjected to TAC, therefore we performed TUNEL assays to assess cardiac apoptosis (Figs. 4H & I). We observed significantly increased TUNEL positive nuclei in LV sections from AKAP-Lbc-ΔPKD mice compared to WT mice subjected to TAC. Average TUNEL positive nuclei content (± SEM) was 0.60 ± 0.06 % for WT/TAC and 1.63 ± 0.10 % for AKAP-Lbc-ΔPKD/TAC ($p<0.001$, n=1000 cells/group).

Overall, in response to TAC-induced pressure overload, AKAP-Lbc-ΔPKD mice exhibit reduced myocyte hypertrophy and cellularity, with increased extracellular space, fibrosis and apoptosis, thereby contributing to the reduced cardiac function observed when compared to WT mice subjected to TAC.

3.5. AKAP-Lbc-ΔPKD mice exhibit reduced histone deacetylase 5 (HDAC5) phosphorylation and hypertrophic gene expression and in response to TAC-induced pressure overload or AT-II/PE infusion

Previously, using cultured neonatal rat ventricular myocytes *in vitro*, we demonstrated that activation of PKD1 through AKAP-Lbc facilitates phosphorylation and subsequent nuclear export of histone deacetylase 5 (HDAC5) [21]. This leads to de-repression of the

transcription factor MEF2, resulting in cardiac myocyte hypertrophy through MEF2-mediated transcription of muscle-specific genes and re-expression of “fetal” developmental genes [29]. Therefore we examined this signaling pathway *in vivo* in AKAP-Lbc-ΔPKD mice compared to WT control mice, to determine the role of AKAP-Lbc-PKD1 in the context of pathological hypertrophy, remodeling and the development of heart failure in an animal model.

We measured total PKD specific activity in heart lysates from AKAP-Lbc-ΔPKD and WT mice subjected to TAC or sham surgery (Fig. 5A). As expected, based on basal PKD activity measurements (Fig. 1F), total PKD specific activity is reduced (~30%) in AKAP-Lbc-ΔPKD/sham compared to WT/sham heart lysates. In response to TAC, PKD specific activity is significantly increased (1.54 ± 0.09 fold) in WT mice heart lysate, however a significant increase in PKD activity is not observed for AKAP-Lbc-ΔPKD mice (1.08 ± 0.04 fold increase).

We next determined levels of HDAC5 phosphorylation (as well as AKAP-Lbc and PKD expression levels) by Western blot using heart lysate from AKAP-Lbc-ΔPKD and control WT mice, in response to TAC (Fig. 5B). Consistent with previous *in vitro* studies [21], AKAP-Lbc expression is upregulated under hypertrophic conditions, in response to TAC. Importantly, HDAC5 phosphorylation is decreased in AKAP-Lbc-ΔPKD mice compared to WT control littermates, in response to TAC. Similar results are observed in response to AT-II/PE treatment (Supp. Fig. 5A). These results suggest that Mef2 transcription will be reduced in the AKAP-Lbc-ΔPKD mice compared to WT control littermates, in response to TAC and AT-II/PE. RT-PCR was performed to examine expression of multiple Mef2-hypertrophic-responsive genes from AKAP-Lbc-ΔPKD and control WT mice cardiac samples, including: atrial natriuretic peptide (ANP) and brain natriuretic peptide (BNP) [41], myofilament proteins; α-actinin, α-myosin heavy chain (α-MHC) and β-myosin heavy chain (β-MHC) [42-44] and isocitrate dehydrogenase (NAD) catalytic subunit 6 (IDH6) (a component of the mitochondrial oxidative phosphorylation chain) [45].

ANP expression is significantly elevated (27.8 ± 7.5 fold, $p \leq 0.05$) in WT/TAC mice compared to WT/sham, AKAP-Lbc-ΔPKD/sham, and AKAP-Lbc-ΔPKD/TAC mice. No statistically significant difference in ANP expression is observed between AKAP-Lbc-ΔPKD/sham and AKAP-Lbc-ΔPKD/TAC (Fig. 5C). BNP expression is increased in WT/TAC and AKAP-Lbc-ΔPKD/TAC compared to sham mice. Interestingly, BNP expression is significantly reduced in AKAP-Lbc-ΔPKD/sham compared to WT/sham mice (0.4 ± 0.03 fold, $p \leq 0.05$; Fig. 5D). α-actinin expression is significantly elevated in WT/TAC mice (1.9 ± 0.04 fold, $p \leq 0.05$) compared to WT/sham, AKAP-Lbc-ΔPKD/sham and AKAP-Lbc-ΔPKD/TAC mice. No significant difference is seen in α-actinin expression between AKAP-Lbc-ΔPKD/sham and AKAP-Lbc-ΔPKD/TAC mice (Fig. 5E). α-MHC expression is not significantly affected in WT/TAC compared to WT/sham. α-MHC expression is slightly elevated in AKAP-Lbc-ΔPKD/sham mice compared to all other groups (1.1 ± 0.02 fold, $p \leq 0.05$), (Fig. 5F). β-MHC expression is significantly increased (18.8 ± 4.8 fold, $p \leq 0.05$) in WT/TAC compared WT/sham, AKAP-Lbc-ΔPKD/sham and AKAP-Lbc-ΔPKD/TAC mice (Fig. 5G). No significant differences are observed in IDH6 expression in all groups (Fig. 5H). Similar results are observed in response to AT-II/PE treatment (Supp. Fig. 5).

Mechanistically, our data indicate that a critical role of AKAP-Lbc in the development of compensatory hypertrophy is due to regulation of PKD1 through AKAP-Lbc, promoting downstream hypertrophic gene expression, which may be mediated at least in part via HDAC5 phosphorylation and Mef2-mediated transcription.

4. DISCUSSION

This study defines an *in vivo* role for AKAP-Lbc in the regulation of pathological cardiac hypertrophy and remodeling under certain conditions of cardiac stress. Unlike the hypertrophic response induced by isoproterenol, via β-adrenergic signaling [30], AKAP-Lbc-ΔPKD mice fail to develop compensatory cardiac hypertrophy in response to chronic AT-II/PE treatment or TAC-induced pressure overload. Collectively, these results indicate that the C-terminus of AKAPLbc, which binds PKD1 and mediates PKD1 signaling is required for the development of compensatory cardiac hypertrophy in response to specific pathways that promote PKD activation, likely downstream of Gq, rather than Gs-Protein-Coupled Receptors, such as the β-adrenergic receptor.

Mechanistically, in accordance with our previous *in vitro* studies [21], we demonstrate that loss of AKAP-Lbc-regulated PKD1 signaling results in reduced HDAC5 phosphorylation in response to TAC (Fig. 5B) or AT-II/PE treatment (Supp. Fig. 5A). Thus, a compensatory hypertrophic response is not properly initiated in AKAP-Lbc-ΔPKD mice, presumably at least in part due to lack of de-repression of Mef2-transcriptional activity, which is induced by phosphorylation and subsequent nuclear export of HDAC5 [28] [29].

Given our current understanding of AKAP-Lbc and the key roles of PKD1 in cardiac signaling, we have specifically focused on AKAP-Lbc-PKD1 signal transduction in this report. PKD1 is emerging as a key player in cardiac signaling. Under pathological conditions, PKD1 plays a key role in altered gene expression, hypertrophy and cardiac remodeling underlying heart failure [26] [29]. PKD1 also functions to regulate Ca^{2+}-handling [46-48], sarcomeric dynamics and cardiac contractility [49] [50], and may play a cardioprotective role under conditions of oxidative stress [51-54]. Despite identification of these vital cardiac functions, it is not well understood how PKD1 is regulated in the heart [55], which is vital for understanding and treatment of cardiac disease. Our data provide unique insight into PKD1-mediated pathophysiological mechanisms, demonstrating *in vivo* that PKD1 interaction with AKAP-Lbc is crucial for the spatial and contextual regulation of PKD1.

Importantly, we have characterized the AKAP-Lbc-ΔPKD mice, demonstrating that PKD1 binding to AKAP-Lbc and AKAP-Lbc-associated PKD activity is abolished (Fig. 1D), whereas AKAP-Lbc-PKA binding and associated activity is unaffected (Fig. 1E). Additionally, we demonstrate that total cardiac PKD activity (not expression level) is reduced (Fig. 1F), but not total cardiac PKA activity or AKAP-Lbc Rho GEF activity. It should however be noted that deletion of the AKAP-Lbc C-terminus may affect not only PKD1, but possibly also other as yet undefined signaling pathways.

By extending our studies to an *in vivo* model we now have a key understanding of the pathophysiological role of AKAP-Lbc in response to cardiac stress and the development of heart failure. Our data clearly indicates that compensatory hypertrophy is blocked in AKAP-Lbc-ΔPKD mice in response to TAC and AT-II/PE treatment, demonstrating an essential compensatory role for the AKAP-Lbc C-terminus, PKD-binding region under certain stress conditions. Unlike WT control littermates, which display increased myocyte growth, increased systolic function with preserved diastolic relaxation, in response to pressure overload or chronic AT-II/PE stimulation, AKAP-Lbc-ΔPKD mice fail to develop these adaptive modifications, thereby accelerating progression to heart failure (Figs. 2, 3 and Supp. Figs. 1-3). AKAP-Lbc-ΔPKD mice also exhibit increased cardiac fibrosis and interstitial collagen content compared to WT mice, in response to TAC (Fig. 4) or AT-II/PE treatment (Supp. Fig 4). This is likely to be a key factor contributing to the cardiac dysfunction observed in AKAP-Lbc-ΔPKD mice [56]. Our results implicate AKAP-Lbc in cardiac fibrosis, suggesting that the C-terminus of AKAP-Lbc and AKAP-Lbc-regulated PKD1 play a role in regulating collagen production and distribution in the heart. In other studies, mice with a cardiac-specific deletion of PKD1 exhibit diminished fibrosis in response to pressure overload or chronic AT-II treatment, suggesting that PKD1 activity promotes fibrosis [57]. Intriguingly, in mice with cardiac myocyte-specific transgenic over-expression of a constitutively active mutant of PKD1, robust ventricular fibrosis was readily detected, but myocardial collagen content was significantly reduced in response to severe thoracic aortic banding [58]. In light of these data, we postulate that loss of AKAP-Lbc-regulated PKD1 leads to reduced and mis-regulated PKD1 activity in cardiac myocytes and/or fibroblasts, resulting in increased fibrosis and collagen content in the hearts of AKAP-Lbc-ΔPKD mice in response to TAC and AT-II/PE treatment. A mechanistic role for PKD1 signaling in cardiac fibroblasts, myofibroblasts and in development of fibrosis is currently undefined, therefore we are investigating this further.

AKAP-Lbc-ΔPKD mice display increased susceptibility to cell death in response to TAC (Figs. 4H & I), suggesting that AKAP-Lbc-PKD1 enhances cardiac myocyte survival, regulating programmed cell death and protection from apoptosis in response to TAC-induced pressure overload. Interestingly, a cardioprotective role for PKD1 has recently been reported downstream of RhoA, in response to ischemia/reperfusion [54], however mechanistically, it is unclear how PKD1 is regulated and downstream signaling is yet to be determined. Given that AKAP-Lbc scaffolds PKD1 and also functions as a guanine exchange factor for Rho, the cardiac role of AKAP-Lbc under conditions of oxidative stress is an exciting area for future investigation. Interestingly, a recent report by Del Vescovo et al., describes an interaction between AKAP-Lbc and IKKβ, a crucial regulator of the transcription factor nuclear factor (NF)-κB, that promotes NFκB-dependent production of interleukin-6 (IL6), which enhances fetal gene expression and cardiomyocyte growth [18].

5. CONCLUSION

In summary, we have demonstrated a critical *in vivo* role for AKAP-Lbc in the development of compensatory hypertrophy, in part, by mediating PKD1 phosphorylation of HDAC5, and promoting hypertrophic gene transcription to enhance cardiac performance in response to TAC-induced pressure overload and AT-II/PE treatment. Functionally, AKAP-Lbc-PKD1

signaling acts to reduce the development of cardiac fibrosis, apoptosis and the development of heart failure.

Supplementary Material

Refer to Web version on PubMed Central for supplementary material.

Acknowledgments

We thank Dr. Robert Gaffin (the UIC CCVR Physiology Core) for help with TAC and blood pressure measurements, and Dr. Matthew Curtis (UIC RRC Imaging Core) for help with microscopy.

7. SOURCES OF FUNDING

This study was supported by American Heart Association Grant 11SDG5230003 to GKC and National Center for Advancing Translational Science - UIC Center for Clinical and Translational Sciences Grant UL1TR000050. BTB was supported by National Institutes of Health (NIH) T32 Training Grant 5T32HL072742-09 through the University of Illinois at Chicago Department of Cardiology. MMM was supported by NIH grants T32 HL07692-16-20 and F32 HL116094. KB was supported by NIH grants HL089617 and HL089617-03S1. BRC was supported by NIH grants GM080223, HG003053 and HL66621.

Non-standard Abbreviations and Acronyms

1M	one month
AT-II	angiotensin II
E/A ratio	early (E) to late (atrial - A) ventricular filling velocity ratio
EDT	transmitral early filling deceleration time
EDV	end-diastolic volume
EF	ejection fraction ET-1, endothelin-1
FS	fractional shortening
GPCR	G protein coupled receptor HDAC5, histone deacetylase 5
HOP	hydroxyproline
HW/BW	heart weight to body weight ratio
LV	left ventricular/ventricle
LVAWD	left ventricular diastolic anterior wall thickness
LVPWD	left ventricular diastolic posterior wall thickness
PE	phenylephrine PKA, protein kinase A
PKC	protein kinase C PKD, protein kinase D
TAC	transverse aortic constriction
WT	wild type

REFERENCES

1. Chien KR, Olson EN. Converging pathways and principles in heart development and disease. Cell. 2002; 110(2):153–162. [PubMed: 12150924]
2. Mudd JO, Kass DA. Tackling heart failure in the twenty-first century. Nature. 2008; 451(7181): 919–928. [PubMed: 18288181]
3. Carnegie GK, Means CK, Scott JD. A-kinase anchoring proteins: from protein complexes to physiology and disease. IUBMB Life. 2009; 61(4):394–406. [PubMed: 19319965]
4. Mauban JR, O'Donnell M, Warrier S, Manni S, Bond M. AKAP-scaffolding proteins and regulation of cardiac physiology. Physiology (Bethesda). 2009; 24:78–87. [PubMed: 19364910]
5. Carnegie GK, Burmeister BT. A-kinase anchoring proteins that regulate cardiac remodeling. J Cardiovasc Pharmacol. 2011; 58(5):451–458. [PubMed: 22075671]
6. Hulme JT, Lin TW, Westenbroek RE, Scheuer T, Catterall WA. Beta-adrenergic regulation requires direct anchoring of PKA to cardiac CaV1.2 channels via a leucine zipper interaction with A kinase-anchoring protein 15. Proc Natl Acad Sci U S A. 2003; 100(22):13093–13098. [PubMed: 14569017]
7. Lygren B, Carlson CR, Santamaria K, Lissandron V, McSorley T, Litzenberg J, et al. AKAP complex regulates Ca2+ re-uptake into heart sarcoplasmic reticulum. EMBO Rep. 2007; 8(11): 1061–1067. [PubMed: 17901878]
8. Kapiloff MS, Schillace RV, Westphal AM, Scott JD. mAKAP: an A-kinase anchoring protein targeted to the nuclear membrane of differentiated myocytes. J. Cell Sci. 1999; 112(Pt 16):2725–2736. [PubMed: 10413680]
9. Russell MA, Lund LM, Haber R, McKeegan K, Cianciola N, Bond M. The intermediate filament protein, synemin, is an AKAP in the heart. Arch Biochem Biophys. 2006; 456(2):204–215. [PubMed: 16934740]
10. Reynolds JG, McCalmon SA, Tomczyk T, Naya FJ. Identification and mapping of protein kinase A binding sites in the costameric protein myospryn. Biochim Biophys Acta. 2007; 1773(6):891–902. [PubMed: 17499862]
11. Sumandea CA, Garcia-Cazarin ML, Bozio CH, Sievert GA, Balke CW, Sumandea MP. Cardiac troponin T, a sarcomeric AKAP, tethers protein kinase A at the myofilaments. J Biol Chem. 2011; 286(1):530–541. [PubMed: 21056973]
12. Aye TT, Soni S, van Veen TA, van der Heyden MA, Cappadona S, Varro A, et al. Reorganized PKA-AKAP associations in the failing human heart. J Mol Cell Cardiol. 2011
13. Diviani D, Soderling J, Scott JD. AKAP-Lbc anchors protein kinase A and nucleates Galpha 12-selective Rho-mediated stress fiber formation. J. Biol. Chem. 2001; 276(47):44247–44257. [PubMed: 11546812]
14. Toksoz D, Williams DA. Novel human oncogene lbc detected by transfection with distinct homology regions to signal transduction proteins. Oncogene. 1994; 9(2):621–8. [PubMed: 8290273]
15. Carnegie GK, Smith FD, McConnachie G, Langeberg LK, Scott JD. AKAP-Lbc nucleates a protein kinase D activation scaffold. Mol. Cell. 2004; 15:889–899. [PubMed: 15383279]
16. Cariolato L, Cavin S, Diviani D. A-kinase anchoring protein (AKAP)-Lbc anchors a PKN-based signaling complex involved in alpha1-adrenergic receptor-induced p38 activation. J Biol Chem. 2011; 286(10):7925–7937. [PubMed: 21224381]
17. Smith FD, Langeberg LK, Cellurale C, Pawson T, Morrison DK, Davis RJ, et al. AKAP-Lbc enhances cyclic AMP control of the ERK1/2 cascade. Nat Cell Biol. 2010; 12(12):1242–1249. [PubMed: 21102438]
18. Del Vescovo CD, Cotecchia S, Diviani D. Akap-Lbc anchors IKKbeta to support interleukin-6-mediated cardiomyocyte hypertrophy. Mol Cell Biol. 2012
19. Burmeister BT, Taglieri DM, Wang L, Carnegie GK. SH2 domain-containing phosphatase 2 (Shp2) is a component of the AKAP-Lbc complex and is inhibited by protein kinase A (PKA) under pathological hypertrophic conditions in the heart. J Biol Chem. 2012

20. Mayers CM, Wadell J, McLean K, Venere M, Malik M, Shibata T, et al. The Rho guanine nucleotide exchange factor AKAP13 (BRX) is essential for cardiac development in mice. J Biol Chem. 2010; 285(16):12344–12354. [PubMed: 20139090]
21. Carnegie GK, Soughayer J, Smith FD, Pedroja BS, Zhang F, Diviani D, et al. AKAP-Lbc mobilizes a cardiac hypertrophy signaling pathway. Mol Cell. 2008; 32(2):169–179. [PubMed: 18951085]
22. Appert-Collin A, Cotecchia S, Nenniger-Tosato M, Pedrazzini T, Diviani D. The A-kinase anchoring protein (AKAP)-Lbc-signaling complex mediates alpha1 adrenergic receptor-induced cardiomyocyte hypertrophy. Proc Natl Acad Sci U S A. 2007; 104(24):10140–10145. [PubMed: 17537920]
23. Heineke J, Molkentin JD. Regulation of cardiac hypertrophy by intracellular signalling pathways. Nat Rev Mol Cell Biol. 2006; 7(8):589–600. [PubMed: 16936699]
24. Hill JA, Olson EN. Cardiac plasticity. N Engl J Med. 2008; 358(13):1370–1380. [PubMed: 18367740]
25. Haworth RS, Goss MW, Rozengurt E, Avkiran M. Expression and activity of protein kinase D/protein kinase C mu in myocardium: evidence for alpha1-adrenergic receptor- and protein kinase C-mediated regulation. J Mol Cell Cardiol. 2000; 32(6):1013–1023. [PubMed: 10888254]
26. Avkiran M, Rowland AJ, Cuello F, Haworth RS. Protein kinase d in the cardiovascular system: emerging roles in health and disease. Circ Res. 2008; 102(2):157–163. [PubMed: 18239146]
27. Bossuyt J, Chang CW, Helmstadter K, Kunkel MT, Newton AC, Campbell KS, et al. Spatiotemporally distinct PKD activation in adult cardiomyocytes in response to phenylephrine and endothelin. J Biol Chem. 2011
28. McKinsey TA, Zhang CL, Olson EN. Identification of a signal-responsive nuclear export sequence in class II histone deacetylases. Mol Cell Biol. 2001; 21(18):6312–6321. [PubMed: 11509672]
29. Vega RB, Harrison BC, Meadows E, Roberts CR, Papst PJ, Olson EN, et al. Protein kinases C and D mediate agonist-dependent cardiac hypertrophy through nuclear export of histone deacetylase 5. Mol Cell Biol. 2004; 24(19):8374–8385. [PubMed: 15367659]
30. Spindler MJ, Burmeister BT, Huang Y, Hsiao EC, Salomonis N, Scott MJ, et al. AKAP13 Rho-GEF and PKD-binding domain deficient mice develop normally but have an abnormal response to β-adrenergic-induced cardiac hypertrophy. PLoS ONE. Apr 26.2013 8(4)
31. Skarnes WC. Gene trapping methods for the identification and functional analysis of cell surface proteins in mice. Methods Enzymol. 2000; 328:592–615. [PubMed: 11075368]
32. Hastie CJ, McLauchlan HJ, Cohen P. Assay of protein kinases using radiolabeled ATP: a protocol. Nat Protoc. 2006; 1(2):968–971. [PubMed: 17406331]
33. Tanabe S, Kreutz B, Suzuki N, Kozasa T. Regulation of RGS-RhoGEFs by Galpha12 and Galpha13 proteins. Methods Enzymol. 2004; 390:285–294. [PubMed: 15488184]
34. DeSantiago J, Bare DJ, Semenov I, Minshall RD, Geenen DL, Wolska BM, et al. Excitation-contraction coupling in ventricular myocytes is enhanced by paracrine signaling from mesenchymal stem cells. J Mol Cell Cardiol. 2012; 52(6):1249–56. [PubMed: 22465692]
35. Taglieri DM, Monasky MM, Knezevic I, Sheehan KA, Lei M, Wang X, et al. Ablation of p21-activated kinase-1 in mice promotes isoproterenol-induced cardiac hypertrophy in association with activation of Erk1/2 and inhibition of protein phosphatase 2A. J Mol Cell Cardiol. 2011; 51(6):988–996. [PubMed: 21971074]
36. deAlmeida AC, van Oort RJ, Wehrens XH. Transverse aortic constriction in mice. J Vis Exp. 2010; (38)
37. Picard MH, Adams D, Bierig SM, Dent JM, Douglas PS, Gillam LD, et al. American Society of Echocardiography recommendations for quality echocardiography laboratory operations. J Am Soc Echocardiogr. 2011; 24(1):1–10. [PubMed: 21172594]
38. Schmittgen TD, Livak KJ. Analyzing real-time PCR data by the comparative C(T) method. Nat Protoc. 2008; 3(6):1101–8. [PubMed: 18546601]
39. Baisamy L, Jurisch N, Diviani D. Leucine zipper-mediated homo-oligomerization regulates the Rho-GEF activity of AKAP-Lbc. J Biol Chem. Apr 15; 2005 280(15):15405–12. [PubMed: 15691829]

40. Hong KW, Lim JE, Oh B. A regulatory SNP in AKAP13 is associated with blood pressure in Koreans. J Hum Genet. Mar; 2011 56(3):205–10. [PubMed: 21228793]
41. Christoffersen TE, Aplin M, Strom CC, Sheikh SP, Skott O, Busk PK, et al. Increased natriuretic peptide receptor A and C gene expression in rats with pressure-overload cardiac hypertrophy. Am J Physiol Heart Circ Physiol. Apr; 2006 290(4):H1635–41. [PubMed: 16272201]
42. Schwartz K, Carrier L, Chassagne C, Wisnewsky C, Boheler KR. Regulation of myosin heavy chain and actin isogenes during cardiac growth and hypertrophy. Symp Soc. Exp. Biol. 1992; 46:265–272. [PubMed: 1341040]
43. Dorn GW 2nd, Robbins J, Ball N, Walsh RA. Myosin heavy chain regulation and myocyte contractile depression after LV hypertrophy in aortic-banded mice. Am J Physiol Heart Circ Physiol. 1994; 267(1):H400–H405.
44. Potthoff MJ, Olson EN. MEF2: a central regulator of diverse developmental programs. Development. Dec. 2007; 134(23):4131–40. [PubMed: 17959722]
45. el Azzouzi H, van Oort RJ, van der Nagel R, Sluiter W, Bergmann MW, De Windt LJ. MEF2 transcriptional activity maintains mitochondrial adaptation in cardiac pressure overload. Eur J Heart Fail. Jan; 2010 12(1):4–12. [PubMed: 20023039]
46. Goodall MH, Wardlow RD 2nd, Goldblum RR, Ziman A, Lederer WJ, Randall W, et al. Novel function of cardiac protein kinase D1 as a dynamic regulator of Ca2+ sensitivity of contraction. J Biol Chem. 2010; 285(53):41686–41700. [PubMed: 21041300]
47. Aita Y, Kurebayashi N, Hirose S, Maturana AD. Protein kinase D regulates the human cardiac L-type voltage-gated calcium channel through serine 1884. FEBS Lett. 2011; 585(24):3903–3906. [PubMed: 22100296]
48. Koncz P, Szanda G, Fulop L, Rajki A, Spat A. Mitochondrial Ca2+ uptake is inhibited by a concerted action of p38 MAPK and protein kinase D. Cell Calcium. 2009; 46(2):122–129. [PubMed: 19631981]
49. Bardswell SC, Cuello F, Rowland AJ, Sadayappan S, Robbins J, Gautel M, et al. Distinct sarcomeric substrates are responsible for protein kinase D-mediated regulation of cardiac myofilament Ca2+ sensitivity and cross-bridge cycling. J Biol Chem. 2010; 285(8):5674–5682. [PubMed: 20018870]
50. Cuello F, Bardswell SC, Haworth RS, Yin X, Lutz S, Wieland T, et al. Protein kinase D selectively targets cardiac troponin I and regulates myofilament Ca2+ sensitivity in ventricular myocytes. Circ Res. 2007; 100(6):864–873. [PubMed: 17322173]
51. Ozgen N, Guo J, Gertsberg Z, Danilo P Jr. Rosen MR, Steinberg SF. Reactive oxygen species decrease cAMP response element binding protein expression in cardiomyocytes via a protein kinase D1-dependent mechanism that does not require Ser133 phosphorylation. Mol Pharmacol. 2009; 76(4):896–902. [PubMed: 19620255]
52. Storz P, Doppler H, Toker A. Protein kinase D mediates mitochondrion-to-nucleus signaling and detoxification from mitochondrial reactive oxygen species. Mol Cell Biol. 2005; 25(19):8520–8530. [PubMed: 16166634]
53. Stetler RA, Gao Y, Zhang L, Weng Z, Zhang F, Hu X, et al. Phosphorylation of HSP27 by protein kinase D is essential for mediating neuroprotection against ischemic neuronal injury. J Neurosci. 2011; 32(8):2667–2682. [PubMed: 22357851]
54. Xiang SY, Vanhoutte D, Del Re DP, Purcell NH, Ling H, Banerjee I, et al. RhoA protects the mouse heart against ischemia/reperfusion injury. J Clin Invest. 2011; 121(8):3269–3276. [PubMed: 21747165]
55. Steinberg SF. Regulation of protein kinase D1 activity. Mol Pharmacol. 2012; 81(3):284–291. [PubMed: 22188925]
56. Baicu CF, Stroud JD, Livesay VA, Hapke E, Holder J, Spinale FG, et al. Changes in extracellular collagen matrix alter myocardial systolic performance. Am J Physiol Heart Circ Physiol. 2003; 284(1):H122–132. [PubMed: 12485818]
57. Fielitz J, Kim MS, Shelton JM, Qi X, Hill JA, Richardson JA, et al. Requirement of protein kinase D1 for pathological cardiac remodeling. Proc Natl Acad Sci U S A. 2008; 105(8):3059–3063. [PubMed: 18287012]

58. Massare J, Berry JM, Luo X, Rob F, Johnstone JL, Shelton JM, et al. Diminished cardiac fibrosis in heart failure is associated with altered ventricular arrhythmia phenotype. J Cardiovasc Electrophysiol. 2010; 21(9):1031–1037. [PubMed: 20233273]

HIGHLIGHTS

- We use gene-trap mice expressing a form of AKAP-Lbc unable to bind protein kinase D.
- Cardiac PKD activity is reduced basally and after TAC in AKAP-Lbc-ΔPKD mice.
- ΔPKD mice exhibit diastolic dysfunction and faster progression to heart failure.
- Loss of AKAP-Lbc-PKD1 signaling promotes cardiac fibrosis and apoptosis under stress.
- AKAP-Lbc-PKD1 signaling is key for development of compensatory hypertrophy *in vivo*.

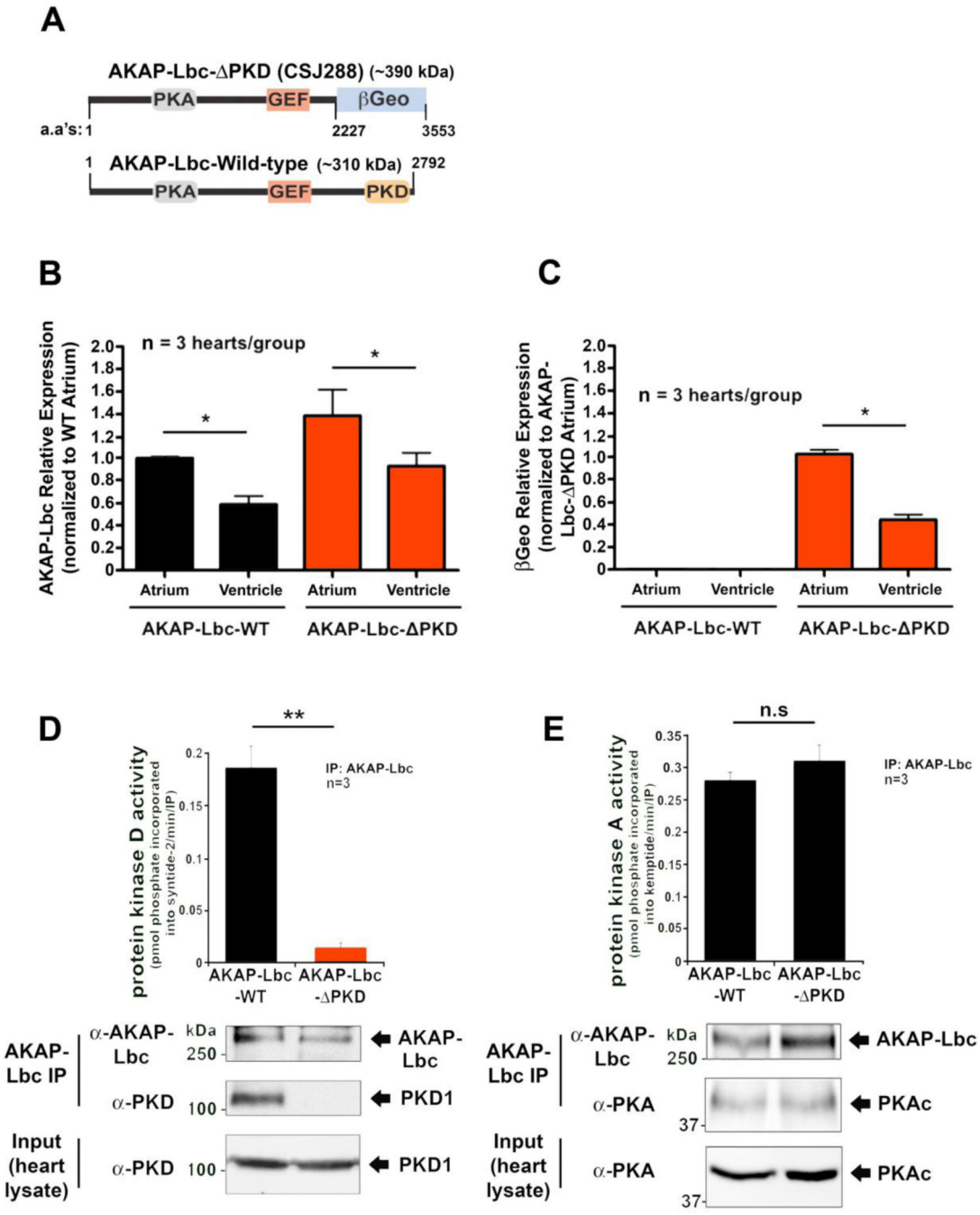

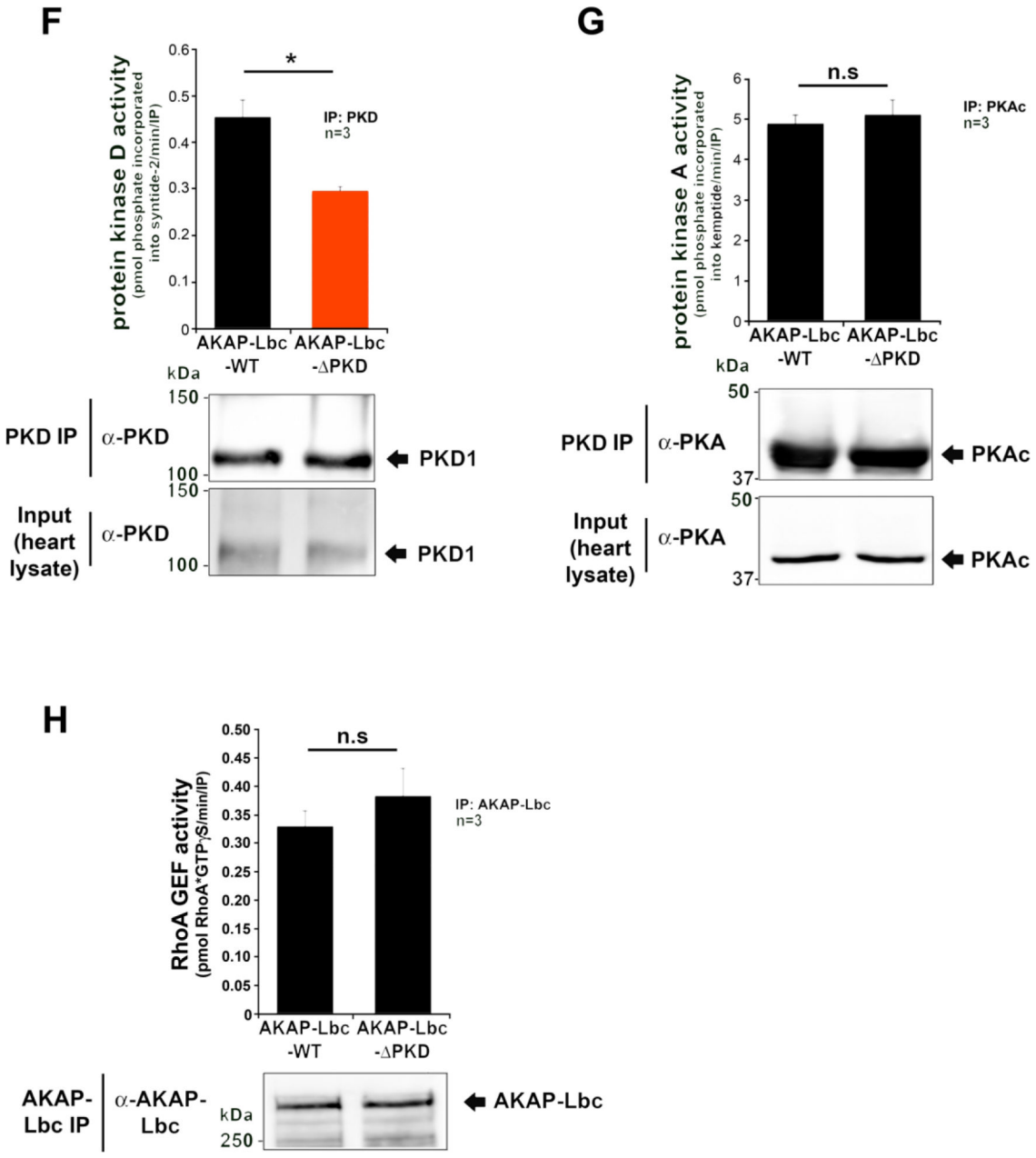

Figure 1. Characterization of AKAP-Lbc-ΔPKD mice

A) Diagram of AKAP-Lbc-ΔPKD (top) and AKAP-Lbc (WT, bottom). AKAP-Lbc-ΔPKD lacks the C-terminus of AKAP-Lbc, where the PKD1 binding region resides, due to fusion of a β-Geo cassette. ***B)*** Quantification of AKAP-Lbc-WT and AKAP-Lbc-ΔPKD atrial and ventricular expression by RT-PCR using AKAP-Lbc-specific primers 6485 forward and 6560 reverse. ***C)*** Control RT-PCR quantifying AKAP-Lbc-ΔPKD atrial and ventricular expression using βGeo-specific primers. ***D)*** AKAP-Lbc-PKD binding is abolished and associated activity is significantly reduced in AKAP-Lbc-ΔPKD mice, compared to WT mice. Endogenous AKAP-Lbc was immunoprecipitated from heart lysate and associated PKD activity was measured by *in vitro* kinase assay. Results presented show mean kinase

activity per IP ± SEM after control IgG IP background activity has been subtracted. Western blot shows corresponding levels of AKAPLbc and PKD in samples and lysates used for PKD activity measurement. ***E)*** AKAP-Lbc-PKA binding and associated PKA activity is similar in AKAP-Lbc-ΔPKD mice, compared to WT mice. Endogenous AKAP-Lbc was immunoprecipitated from heart lysate and associated PKA activity was measured by *in vitro* kinase assay. Western blot shows corresponding levels of AKAP-Lbc and PKA (PKAc; catalytic subunit) in samples and lysates used for PKA activity measurement. ***F)*** Total cardiac PKD activity is significantly reduced in AKAP-Lbc-ΔPKD mice, compared to WT mice. Endogenous PKD was immunoprecipitated from heart lysate and kinase activity was measured *in vitro*. Results presented show mean kinase activity per IP ± SEM after control IgG IP background activity has been subtracted. Western blot shows corresponding levels of PKD1 in samples and lysates used for PKD activity measurement. ***G)*** Total cardiac PKA activity is similar in AKAP-Lbc-ΔPKD mice, compared to WT mice. Endogenous PKAc was immunoprecipitated from heart lysate and kinase activity was measured *in vitro*. Results presented show mean kinase activity per IP ± SEM after control IgG IP background activity has been subtracted. Western blot shows corresponding levels of PKAc in samples and lysates used for PKA activity measurement. ***H)*** AKAP-Lbc Rho-GEF activity is similar in AKAP-Lbc-ΔPKD mice, compared to WT mice. Endogenous AKAP-Lbc was immunoprecipitated from heart lysate and RhoA-GEF activity was measured by *in vitro* assay. Western blot shows corresponding levels of AKAP-Lbc in samples used for activity measurement. Differences in quantitative variables were examined by Student's t-test. ** = $p < 0.01$. N.S = no significant difference between groups. All assays were performed in triplicate for 3 independent experiments.

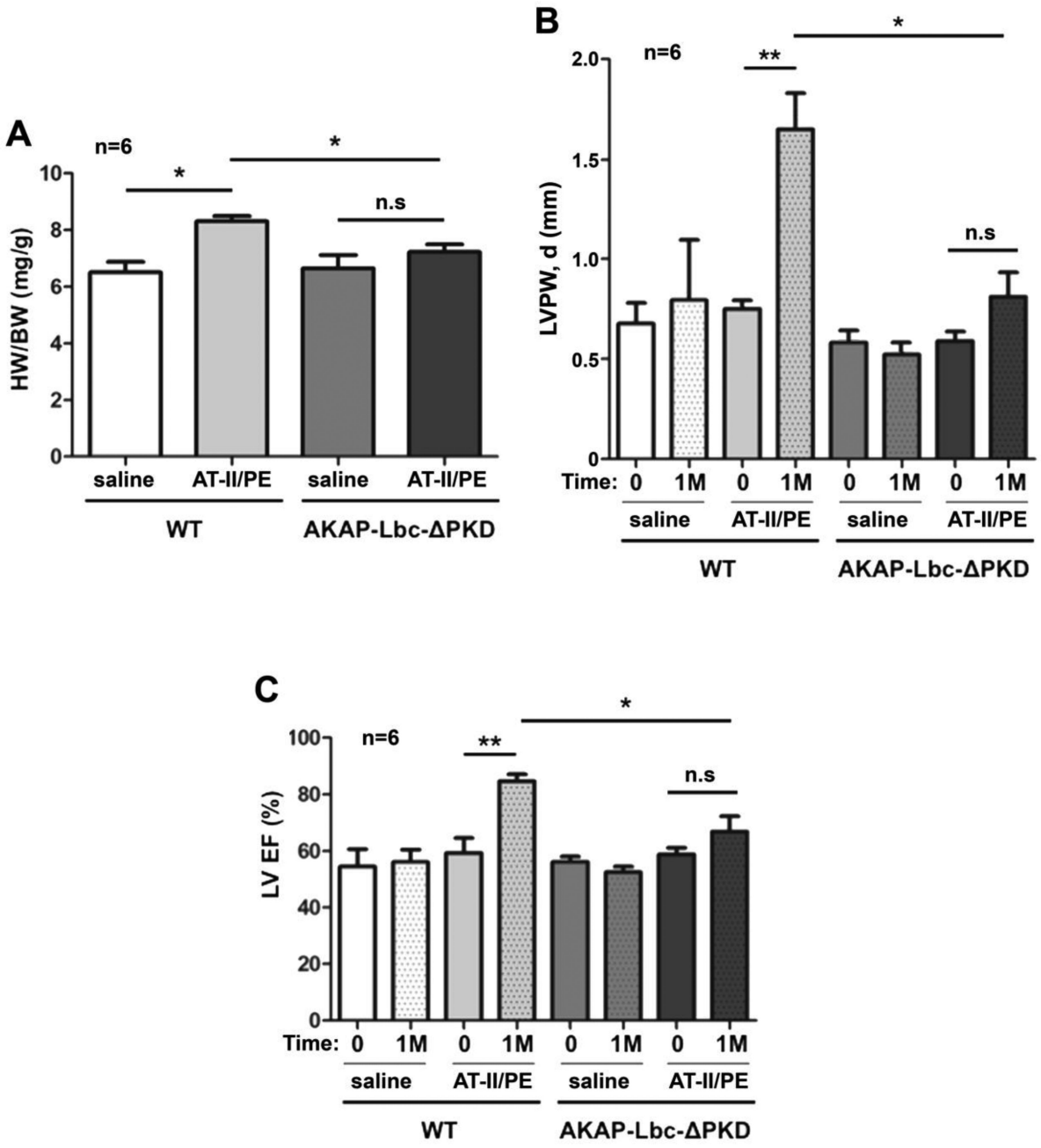

Figure 2. Echocardiographic and gravimetric characteristics of hearts from AKAP-Lbc-ΔPKD mice and control WT littermates, at baseline (0) and after receiving AT-II/PE or saline control for 1 month (1M)

A) WT mice subjected to angiotensin II + phenylephrine for one month (WT + AT-II/PE) develop a significant increase in HW to BW ratio (*$p < 0.05$ WT + AT-II/PE vs. WT + saline); HW to BW ratio for AKAP-Lbc-ΔPKD mice + AT-II/PE is comparable to AKAP-Lbc-ΔPKD mice + saline. HW to BW ratio is significantly increased in WT mice subjected to AT-II/PE compared to AKAPLbc-ΔPKD mice + AT-II/PE (*$p < 0.05$). ***B)*** WT mice + AT-II/PE exhibit an increase in LV Posterior Wall dimension during diastole (LVPW, d), compared to baseline measurements (0) (**$p < 0.01$), and all other groups including AKAP-

Lbc-ΔPKD + AT-II/PE (*p < 0.05). ***C)*** WT + AT-II/PE exhibit an increase in LV Ejection Fraction (EF), compared to baseline measurements (0) (**p < 0.01), and all other groups including AKAP-Lbc-ΔPKD + AT-II/PE (*p < 0.05).

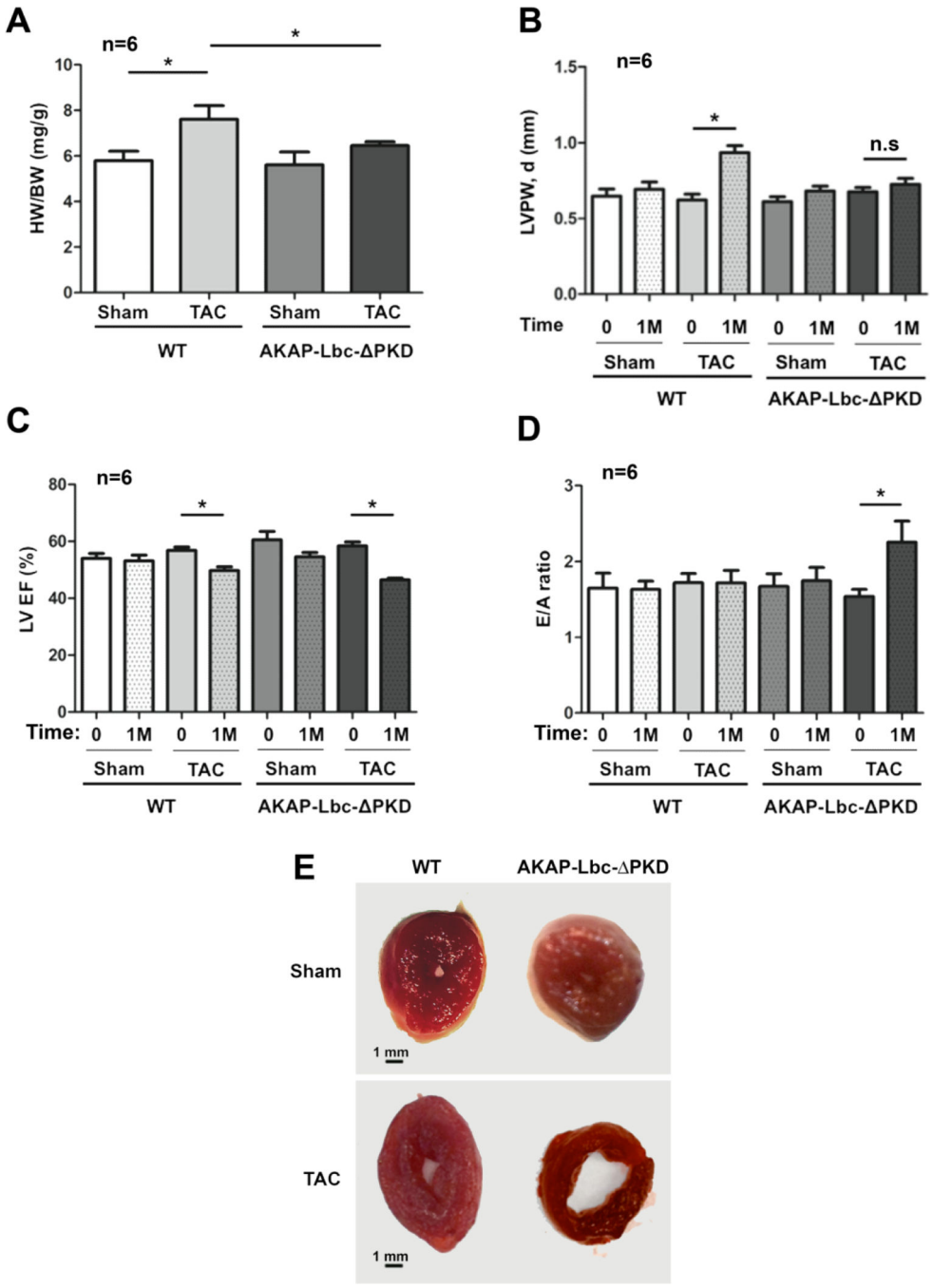

Figure 3. Echocardiographic and gravimetric characteristics of hearts from AKAP-Lbc-ΔPKD mice and control WT littermates, at baseline (0) and after TAC or sham surgery for 1 month (1M)

A) WT mice subjected to TAC for one month develop a significant increase in HW to BW ratio (*p < 0.01 WT/sham vs. WT + TAC); HW to BW ratio for AKAP-Lbc-ΔPKD mice + TAC is comparable to AKAP-Lbc-ΔPKD + sham. HW to BW ratio is increased in WT + TAC compared to AKAP-Lbc-ΔPKD + TAC (*p < 0.05). ***B)*** LV posterior wall thickness in diastole (LVPW,d) is increased in WT + TAC compared to baseline measurements (0), and AKAP-Lbc-ΔPKD mice + TAC. ***C)*** WT + TAC and AKAP-Lbc-ΔPKD + TAC show a

decrease in LV Ejection Fraction (EF), compared to baseline (0) (*p < 0.05). ***D)*** E/A ratio, the early (E) to late (atrial; A) ventricular filling velocity ratio, is significantly increased in AKAP-Lbc-ΔPKD + TAC, compared to WT + TAC, sham and baseline (0) measurements (*p < 0.05). ***E)*** WT and AKAP-Lbc-ΔPKD heart section at the mid-papillary. In response to TAC, WT hearts develop concentric hypertrophy, whereas AKAP-Lbc-ΔPKD hearts exhibit a dilated LV chamber and thin walls.

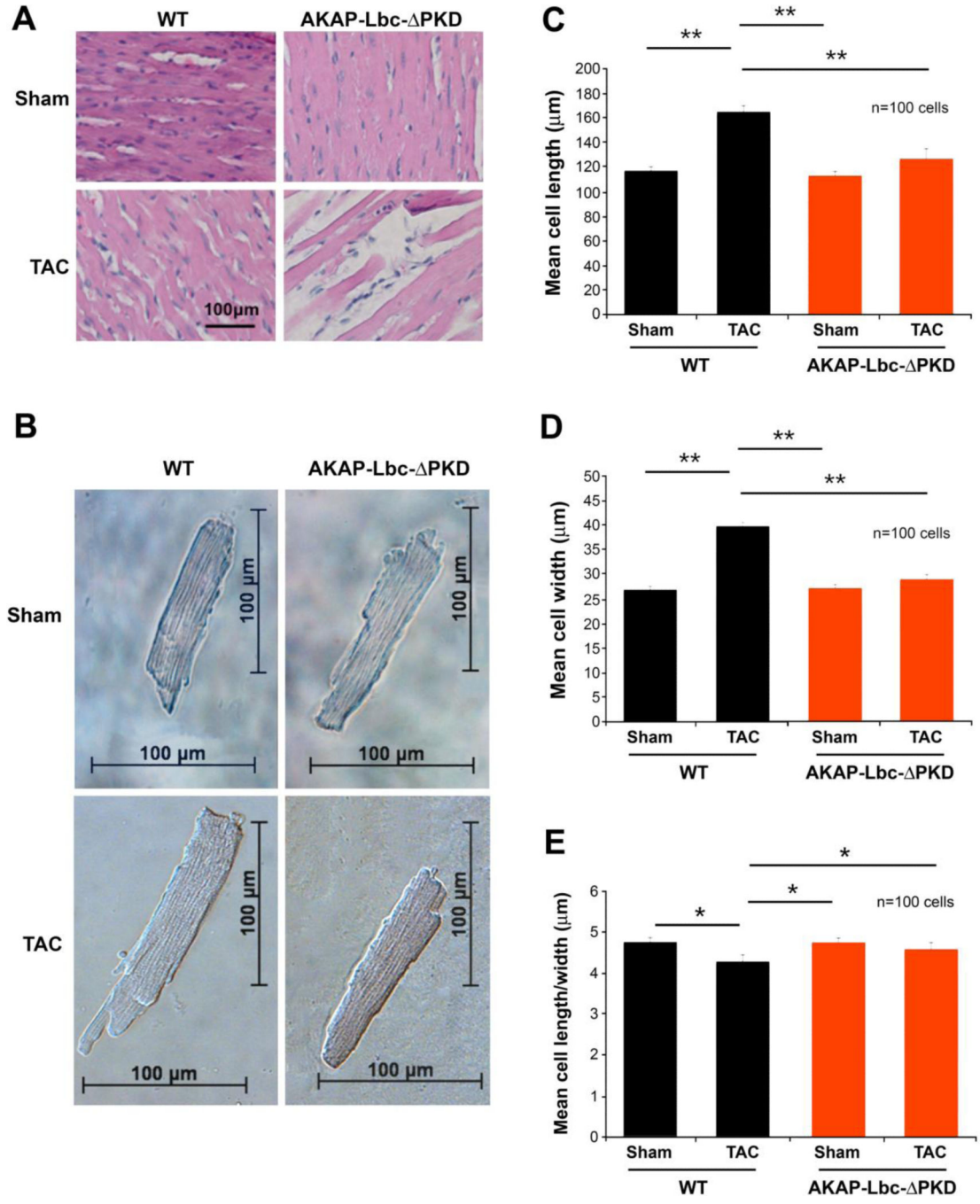

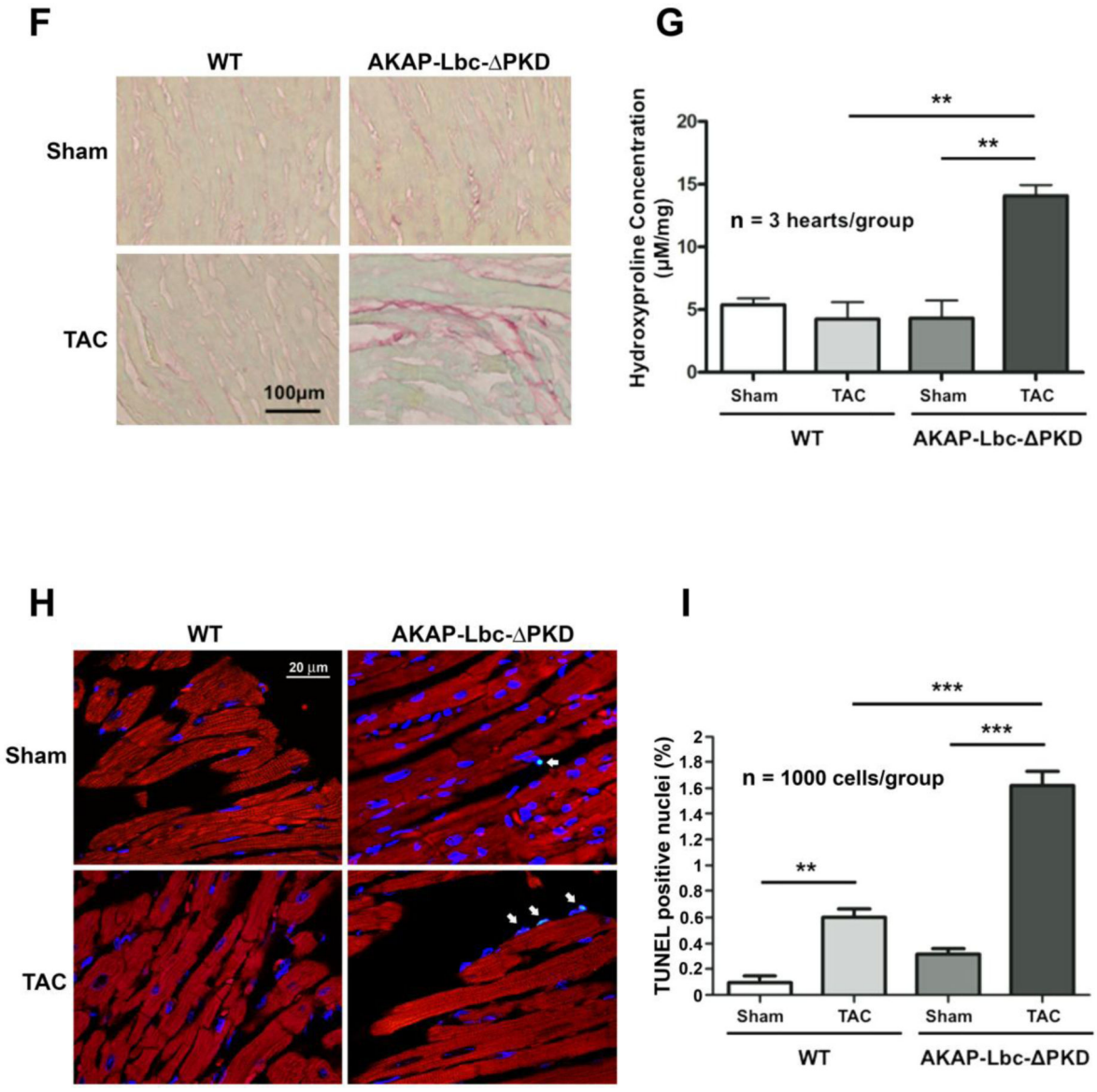

Figure 4. Histological and cellular analysis of WT and AKAP-Lbc-ΔPKD TAC or sham surgery

A) Hematoxylin-Eosin (HE) staining of LV heart sections from WT and AKAP-Lbc-ΔPKD mice after one month of TAC or sham surgery. HE staining shows no difference in the cytoarchitecture of LV heart from control WT and AKAP-Lbc-ΔPKD mice subjected to sham surgery. In response to TAC, WT mice develop cardiomyocyte hypertrophy, whereas AKAPLbc-ΔPKD hearts present with poor cellularity and elongated, thin, myocytes. **(B)** Brightfield images of isolated adult cardiac myocytes. Measurement of **(C)** length **(D)** width and **(E)** length/width ratio of isolated myocytes (n=100 cells). Cell length and width are significantly smaller for AKAP-Lbc-ΔPKD/TAC cardiomyocytes compared to WT/TAC cardiomyocytes (**p<0.01). Length width ratio is increased in AKAP-Lbc-ΔPKD/TAC compared to WT/TAC isolated myocytes (*p<0.05). ***F)*** AKAP-Lbc-ΔPKD mice + TAC show increased extracellular collagen deposition. Sirius-Red staining indicates increased collagen content in hearts from AKAP-Lbc-ΔPKD mice + TAC, compared to all other

groups. ***G)*** Quantification of collagen content in hearts from WT and AKAP-Lbc-ΔPKD mice by hydroxyproline (HOP) assay. Results presented show mean HOP content ± SEM. HOP content in AKAP-Lbc-ΔPKD mice + TAC is significantly higher than all other groups (**$p < 0.01$). All assays were performed using heart samples from 3 different mice for each group. ***H)*** Representative images of TUNEL staining carried out using LV heart sections from WT and AKAP-Lbc-ΔPKD mice subjected to sham or TAC surgery. Apoptotic cells (denoted by arrows) are visualized by incorporation of fluoresceindUTP (green) into fragmented DNA. DAPI staining (blue) is used as a marker for cell nuclei. Sections were co-stained with anti-cTnI (red) to help identify cardiac myocytes. ***I)*** AKAP-Lbc-ΔPKD mice + TAC display a significant increase in apoptosis compared to WT + TAC (***$p < 0.001$). Data represent the mean percentage (± SEM) of apoptotic cells (fluorescein-dUTP positive) from 3 mice per group; 1,000 cells total per group. Differences in quantitative variables were examined by ANOVA.

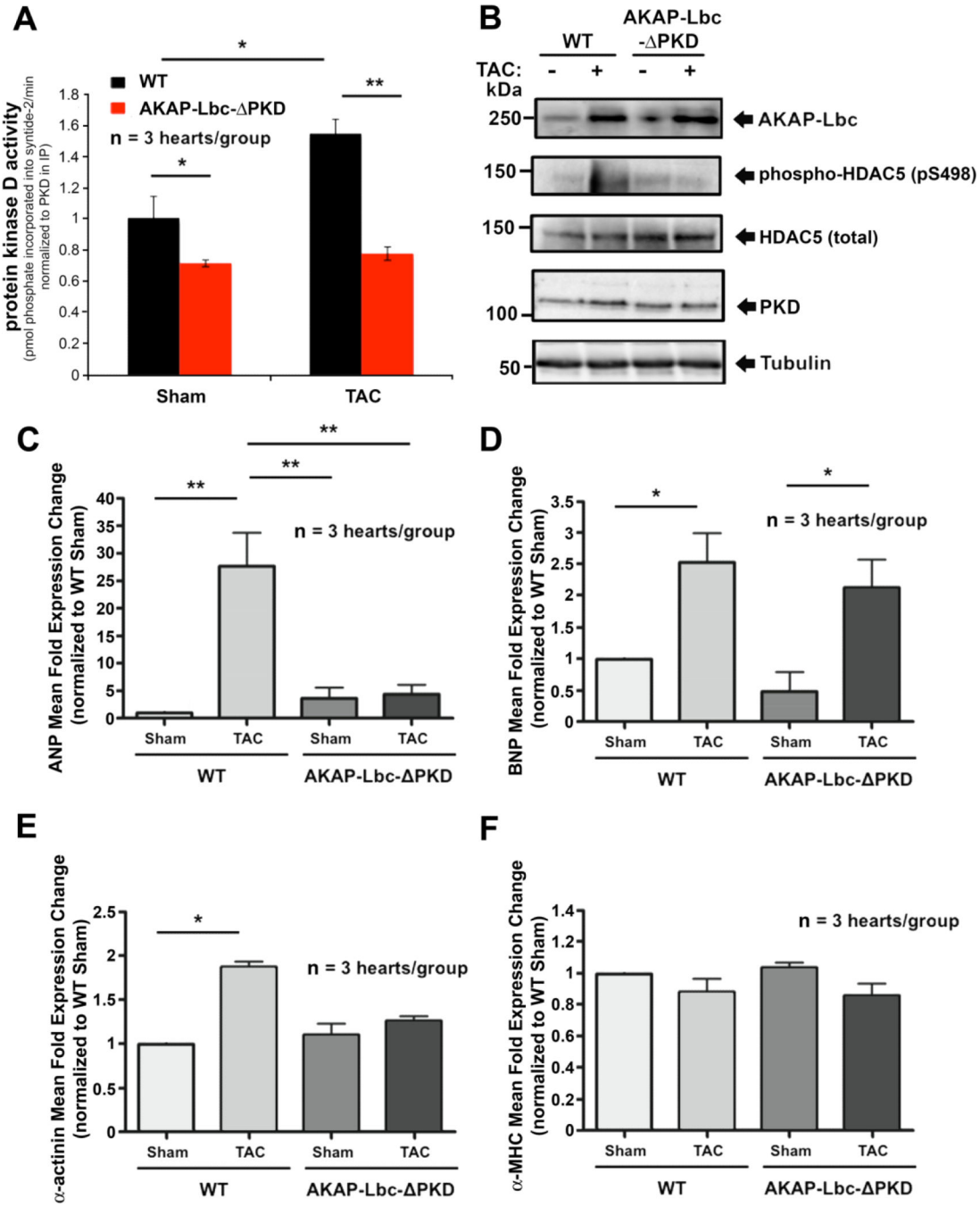

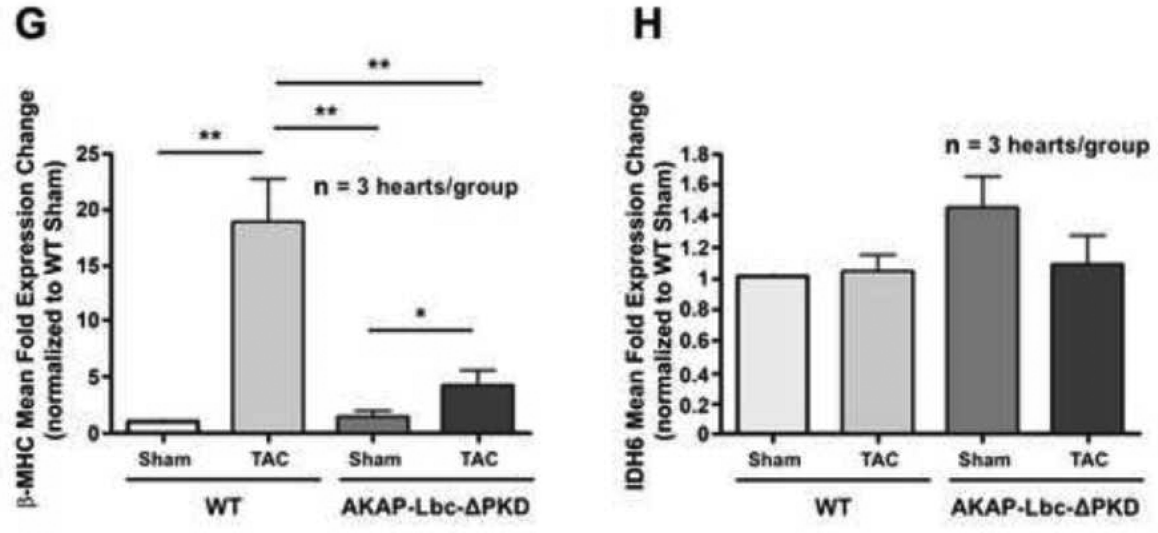

Figure 5. AKAP-Lbc-ΔPKD mice display blunted HDAC5 phosphorylation and reduced hypertrophic gene expression in response to TAC

A) Total cardiac PKD activity is not increased in AKAP-Lbc-ΔPKD mice unlike WT mice, in response to TAC-induced pressure overload. Endogenous PKD was immunoprecipitated from heart lysate and kinase activity was measured *in vitro*. Results presented show PKD specific activity (mean kinase activity normalized to PKD expression per IP) ± SEM. ***B)*** Western blotting of whole heart lysates indicates phosphorylation of HDAC5 at Ser498 is increased in WT/TAC mice, compared to all other groups. AKAP-Lbc expression is upregulated in response to TAC. 6 mice were used for each study group. ***C)*** Effects of TAC on hypertrophic gene expression in WT and AKAP-Lbc-ΔPKD mice were determined by quantitative PCR analysis. ANP expression is significantly increased in WT/TAC but not in AKAP-Lbc-ΔPKD/TAC. ***D)*** BNP expression is significantly increased in WT/TAC and AKAP-Lbc-ΔPKD/TAC. ***E)*** α-actinin expression is significantly increased in WT/TAC but not in AKAP-Lbc-ΔPKD/TAC. ***F)*** α-MHC expression is not significantly affected in response to TAC in WT or AKAP-Lbc-ΔPKD mice. ***G)*** β-MHC expression is significantly increased in WT/TAC but only slightly increased in AKAP-Lbc-ΔPKD/TAC. ***H)*** IDH6 expression is not significantly affected in response to TAC in WT or AKAPLbc-ΔPKD mice. For comparison of all groups, results presented show mean fold gene expression ± SEM, normalized to WT/Sham mean gene expression. Differences in quantitative variables were examined by ANOVA. * = $p < 0.05$, ** = $p < 0.01$. 3 mice were used for each study group.